Boundary conditions for a composite model of leptons and quarks

G B Mainland

The Ohio State University at Newark, Newark, OH 43055, USA

E-mail: mainland.1@osu.edu

Abstract. Because the existence of families of elements and hadrons was ultimately understood by the realization that atoms and hadrons are composite, an obvious approach to explaining the existence of lepton and quark families is to assume that the particles in these families are also composite. The mass and spin spectra of leptons and quarks suggest that if these particles are composite, they are most likely bound states of a scalar and spin-1/2 fermion interacting via electrodynamics. However, if they are composite, the bound states must be highly relativistic since in each family the least massive member has a small mass compared with the others. Also, composite leptons and quarks must be extremely tightly bound since no internal structure has ever been conclusively detected. Highly relativistic, bound-state, Bethe-Salpeter solutions of a scalar and a spin-1/2 fermion bound by minimal electrodynamics are discussed. These specific solutions cannot describe leptons or quarks as bound states because the magnitude of the charges of the constituents are an order of magnitude larger than e. The boundary conditions, however, allow solutions when the constituents have charges with magnitudes on the order of e.

1. Introduction

Because the existence of families of elements and hadrons was ultimately understood by the realization that atoms and hadrons are composite, although speculative, as is any physics beyond the standard model, an obvious approach to explaining the existence of lepton and quark families is to assume that the particles in these families are composite. The theoretical high-energy physics community found this circumstantial evidence sufficiently compelling that in the 1970's many physicists devoted substantial effort to constructing a composite model. But by the early 1980's most physicists had quit working on the idea because a mechanism was never discovered that could tightly bind the constituents[1].

The existence of families, the circumstantial evidence that leptons and quarks are composite, is not conclusively corroborated by direct experimental evidence. There are indications that there might be discrepancies between the experimental value of the of the muon g-2 and the value calculated from the standard model[2]. Even if this disagreement between experiment and theory is confirmed, in addition to muon substructure, it could also be explained, for example, by substructure of the W-boson or by the existence of supersymmetric partners of existing particles.

If leptons and quarks are composite, several characteristics that any composite model must possess can be inferred from the mass and spin spectra of leptons and quarks. The masses of these particles satisfy the inequalities $\mathrm{m}_{\mathrm{electron}} \ll \mathrm{m}_{\mathrm{muon}} \ll \mathrm{m}_{\tau}$, $\mathrm{m}_{\mathrm{up}} \ll \mathrm{m}_{\mathrm{charm}} \ll \mathrm{m}_{\mathrm{top}}$ and $\mathrm{m}_{\mathrm{down}} \ll \mathrm{m}_{\mathrm{strange}} \ll \mathrm{m}_{\mathrm{bottom}}$. Since no structure has been conclusively detected for leptons or quarks, any composite system must be very strongly bound. This precludes a composite model where, for example, the electron, muon and tau are successively much more massive because the constituents are successively much more massive. The large differences in the masses of the particles in each family is consistent with strong binding only if the bound system is highly relativistic. In each family the most tightly bound state must be one for which the binding energy is almost equal to the sum of the masses of the constituents. That is, the interaction must create a state that has almost zero energy. The development of supercomputers makes it possible to study such highly relativistic bound states.

Although the existence of families is explained by the atomic model of atoms, the quark model for mesons and baryons and, as discussed here, perhaps a preon model for leptons and quarks, each of the composite models is radically different. In the atomic model, aside from small mass defects, the mass of an atom is the sum of the masses of the constituents. For mesons and baryons most of the mass results from the kinetic energy of the quarks so the mass of a meson or baryon is substantially greater than the sum of the masses of the constituent quarks. If leptons and quarks are highly relativistic bound states, the mass of each lepton or quark is less - and for the least massive particle in each family, much less - than the sum of the masses of the constituents.

To construct a composite model of leptons and quarks, two questions must initially be answered: (a) What particles constituent the system? (b) What interaction binds the system? For simplicity the bound system would likely consist of two or three constituents. If the composite system were comprised of a spin-0 boson and a spin-1/2 fermion, all states would have total angular momentum or spin one-half if all states have zero orbital angular momentum. If the composite system were comprised of three or more constituents, it is difficult to imagine a mechanism that would prevent higher-spin bound states. Thus, the lepton and quark mass and spin spectra suggest that if the leptons and quarks are composite, they are likely relativistic bound states of a spin-0 boson and a spin-1/2 fermion.

Leptons interact gravitationally, weakly and electromagnetically. Among the three, the electromagnetic interaction is the only one that might be able to provide the requisite strong binding. The similarity of the charged-lepton and quark mass spectra and the fact that the two quark families and the charged lepton family each have three members suggests that the same mechanism might be responsible for binding in all four families, a possible scenario when the strong interactions can be neglected. This would be the situation if only the scalar quark constituent interacts strongly. A heretofore unknown interaction might, of course, be responsible for the binding, but assuming the existence of such a force would represent a more speculative and a much more difficult approach.

2. Possible composite model of leptons and quarks

If each of the lepton and quark families is a bound state of a scalar and a spin-1/2 fermion, the four families can be created from two constituent fermions with respective charges q_{f1}, q_{f2} and two constituent scalars with respective charges Q_{s1}, Q_{s2}. The four constituents can combine in four ways to create four bound states or four families. The four charges must satisfy the four constraints in Table 1. Note that for weak-interaction transitions between the two lepton families or between the two quark families, with the choice of charges in Table 1, the W-boson couples to the constituent fermions. In Table 1 there are three independent equations (constraints) and four unknown charges so there are an infinite number of solutions.

Possible charges of the constituents with magnitudes ≤ 2 that are multiples of $\pm 1/3$ are are given in in Table 2. For each solution the charges of both constituent fermions have the same sign and the charges of both constituent scalars have the opposite sign. Thus only a fermion and a scalar can form a bound state.

Table 1. Constraints on constituent charges.

Family	Constituent Fermion Charge	Constituent Boson Charge	Constraint
Electron	q_{f1}	Q_{s1}	$q_{f1} + Q_{s1} = -1$
Neutrino	q_{f2}	Q_{s1}	$q_{f2} + Q_{s1} = 0$
Neg. quarks	q_{f1}	Q_{s2}	$q_{f1} + Q_{s2} = -\frac{1}{3}$
Pos. quarks	q_{f2}	Q_{s2}	$q_{f2} + Q_{s2} = \frac{2}{3}$

Table 2. Possible charges of constituent fermions and scalars.

Constituent Fermion Charges		Constituent Scalar Charges	
q_{f1}	q_{f2}	Q_{s1}	Q_{s2}
1	2	-2	-4/3
2/3	5/3	-5/3	-1
1/3	4/3	-4/3	-2/3
-4/3	-1/3	1/3	1
-5/3	-2/3	2/3	4/3
-2	-1	1	5/3

3. Bethe-Salpeter equation

When a spin-0 field $\phi(x)$, representing a scalar with charge Q_s and mass m_s, interacts via minimal electrodynamics with a spin-1/2 field $\Psi(x)$, representing a fermion with charge q_f and mass m_f, the renormalizable Lagrangian is[3]

$$L =: [(-\imath\partial^\mu - Q_s A^\mu)\phi^\dagger][(\imath\partial_\mu - Q_s A_\mu)\phi] - m_s^2\phi^\dagger\phi + \bar{\Psi}\gamma_\mu(\imath\partial^\mu - q_f A^\mu)\Psi - m_f\bar{\Psi}\Psi - \frac{1}{4}F_{\mu\nu}F^{\mu\nu} - \frac{1}{2}(\partial^\mu A_\mu)^2 :, \quad (1)$$

where $F_{\mu\nu} = \partial_\nu A_\mu - \partial_\mu A_\nu$ and the final term is the gauge-fixing term for the Feynman gauge.

The Bethe-Salpeter equation is used to calculate the properties of the bound state. Since every Feynman diagram contributes to the exact equation, some approximation must be made. Usually only the effect of the lowest-order diagram shown to the right is included. Because of the structure of the Bethe-Salpeter equation, contributions occur from the diagram and iterations of the diagram, which form a ladder with the photon propagator forming the rungs. Thus the approximation is called the ladder approximation.

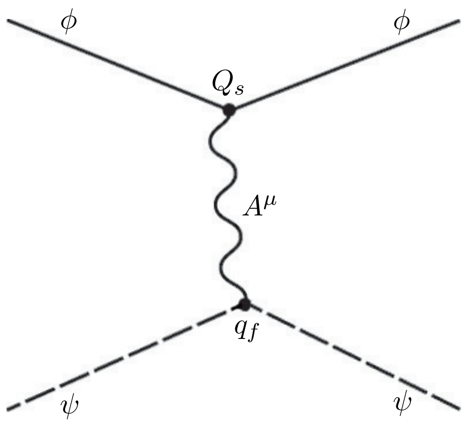

Figure 1. Feynman diagram for a spin-1/2 field ψ with charge q_f and a scalar field ϕ with a charge Q_s interacting with the electromagnetic field A^μ.

Following standard procedures[4] and making the ladder approximation, the Bethe-Salpeter equation describing a bound state of a minimally interacting scalar and spinor is[5]

$$
\begin{aligned}
&[(p^0 + \xi E)\gamma_0 + p^i\gamma_i - m_f]\{[p^0 + (\xi - 1)E]^2 - \mathbf{p}^2 - m_s^2\}\chi(p) \\
&= \frac{iq_f Q_s}{(2\pi)^4} \int_{-\infty}^{\infty} \frac{\mathrm{d}^4 q}{(p-q)^2 + i\varepsilon} \{\gamma^0[p_0 + q_0 + 2(\xi - 1)E] + \gamma^i(p_i + q_i)\}\chi(q)\,. \qquad (2)
\end{aligned}
$$

The equation has been written in the center-of-mass rest frame where the four-momentum K^μ takes the form $K^\mu = (E, 0, 0, 0)$.

In contrast, the non-relativistic, two-body, bound-state problem described by the Schrödinger equation can be written in the form

$$
H(\mathbf{x})\psi(\mathbf{x}) = E\psi(\mathbf{x})\,, \qquad (3)
$$

where H is the Hamiltonian of the system.

Significant differences between bound-state Bethe-Salpeter equation (2) and the bound-state Schrödinger equation (3) are as follows: (a) Since the energy E appears multiple times in the Bethe-Salpeter equation, there is no relativistic operator that has an eigenvalue E. That is, a Hamiltonian does not exist for the relativistic, bound-state problem. (b) The Bethe-Salpeter equation is covariant, implying that there is no action at a distance. If the fourth component of the photon propagator, which is under the integral, were neglected, the interaction would become instantaneous. The interaction would then depend on the distance r between the constituent particles and there would be action at a distance. (c) The Bethe-Salpeter equation is an integral equation so the boundary conditions are part of the equation itself and do not have to be specified independently. (d) Because the energy E appears multiple times in the Bethe-Salpeter equation and the coupling constant $q_f Q_s/(4\pi)$ appears only once, the equation is solved by specifying the energy and solving for the coupling constant as an eigenvalue. When solving the Schrödinger equation, the coupling constant is specified and the energy is calculated as an eigenvalue. Both procedures yield equivalent information that allows the coupling constant to be plotted as a function of the energy or vice versa. (e) The Bethe-Salpeter equation is always separable when energy $E = 0$ because it is invariant under O(3,1) rotations. When the energy is nonzero, only one Bethe-Salpeter equation, the Wick-Cutkosky Model[6, 7], has been separated. (f) When the energy $E = 0$, there are a few analytical solutions of the Bethe-Salpeter equation, but when the energy is nonzero, all solutions are numerical.

Zero-energy solutions, which are the zero-energy limit of finite-energy solutions, are discussed here. Such solutions are important because the structure of the generalized matrix eigenvalue equation that yields zero-energy solutions provides guidance[8] in constructing an appropriate discretized equation when the energy is nonzero.

To obtain solutions to (2) in the limit $E = 0$, the singularity in the kernel is first removed and the equation is transformed from Minkowski to Euclidean space by making a Wick rotation[6], which is always possible in the ladder approximation and is sometimes possible when the effects of higher-order Feynman diagrams are included. The Wick-rotated Bethe-Salpeter equation is

$$
\begin{aligned}
&(\tilde{\gamma}\cdot p + m_f)(p\cdot p + m_s^2)\chi(ip^0, \mathbf{p}) \\
&\qquad = -\frac{q_f Q_s}{(2\pi)^4} \int_{-\infty}^{\infty} \frac{\mathrm{d}^4 q}{(p-q)\cdot(p-q)}\, \tilde{\gamma}\cdot(p+q)\chi(iq^0, \mathbf{q})\,. \qquad (4)
\end{aligned}
$$

In the above equation the Euclidean scalar product $p\cdot p \equiv p^0p^0 + \mathbf{p}\cdot\mathbf{p}$ and $\tilde{\gamma}\cdot p \equiv \tilde{\gamma}^0 p^0 + \tilde{\gamma}^i p^i$. The matrices $\tilde{\gamma}^\mu$ are given by $\tilde{\gamma}^0 \equiv -i\gamma^0, \tilde{\gamma}^i \equiv \gamma^i$.

Dimensionless variables are introduced by defining $m_f \equiv m(1-\Delta), m_s \equiv m(1+\Delta), p' \equiv p/m$ and $q' \equiv q/m$. Writing (4) in terms of dimensionless variables and then omitting primes since all momenta are now dimensionless,

$$\begin{aligned}
&[\tilde{\gamma}\cdot p + (1-\Delta)][p\cdot p + (1+\Delta)^2]\chi(ip^0,\mathbf{p}) \\
&\quad = -\frac{q_f Q_s}{(2\pi)^4}\int_{-\infty}^{\infty}\frac{\mathrm{d}^4 q}{(p-q)\cdot(p-q)}\tilde{\gamma}\cdot(p+q)\chi(iq^0,\mathbf{q})\,.
\end{aligned} \tag{5}$$

Spherical coordinates are introduced as follows:

$$\begin{aligned}
p^0 &= |p|\cos\theta_1 & p_z &= |p|\sin\theta_1\cos\theta_2 \\
p_x &= |p|\sin\theta_1\sin\theta_2\sin\phi & p_y &= |p|\sin\theta_1\sin\theta_2\cos\phi
\end{aligned} \tag{6}$$

The four-vector q is written similarly in terms of primed angles. Then

$$\mathrm{d}^4 q = |q|^3\sin^2\theta_1'\sin\theta_2'\,\mathrm{d}\theta_1'\,\mathrm{d}\theta_2'\,\mathrm{d}\phi'\,\mathrm{d}|q| \equiv |q|^3\mathrm{d}|q|\mathrm{d}\Omega_{(3)}'\,, \tag{7}$$

and

$$(p-q)\cdot(p-q) = |p|^2 + |q|^2 - 2|p|\,|q|\cos\Theta\,, \tag{8}$$

where Θ is the angle between the vectors p and q.

In the zero-energy limit the angular dependence of the equation separates[9, 10] when solutions are written as products of the functions $\Psi_1^{(\pm)}(\theta_1,\theta_2,\phi)$ and $\Psi_2^{(\pm)}(\theta_1,\theta_2,\phi)$ that depend on hyperspherical harmonics in four-dimensional, Euclidean space-time and the functions $F^{(\pm)}(|p|)$ and $G^{(\pm)}(|p|)$ that depend only on the magnitude of the Euclidean four-momentum $|p|$,

$$\chi(ip^0,\mathbf{p}) = F^{(\pm)}(|p|)\Psi_1^{(\pm)}(\theta_1,\theta_2,\phi) + G^{(\pm)}(|p|)\Psi_2^{(\pm)}(\theta_1,\theta_2,\phi)\,. \tag{9}$$

The four-component column vectors $\Psi_1^{(\pm)}(\theta_1,\theta_2,\phi)$ and $\Psi_2^{(\pm)}(\theta_1,\theta_2,\phi)$, which are defined in Ref. 10, are related by

$$\Psi_1^{(-)}(\theta_1,\theta_2,\phi) = \gamma_5\Psi_1^{(+)}(\theta_1,\theta_2,\phi) \quad\text{and}\quad \Psi_2^{(-)}(\theta_1,\theta_2,\phi) = \gamma_5\Psi_2^{(+)}(\theta_1,\theta_2,\phi)\,, \tag{10}$$

and satisfy the relationships

$$\tilde{\gamma}\cdot p\,\Psi_1^{(\pm)}(\theta_1,\theta_2,\phi) = \mp|p|\Psi_2^{(\pm)}(\theta_1,\theta_2,\phi) \quad\text{and}\quad \tilde{\gamma}\cdot p\,\Psi_2^{(\pm)}(\theta_1,\theta_2,\phi) = \pm|p|\Psi_1^{(\pm)}(\theta_1,\theta_2,\phi)\,. \tag{11}$$

After substituting $\chi(ip^0,\mathbf{p})$ as given in (9) with upper superscripts into the Bethe-Salpeter equation (5), the equation can be simplified using (11), and the angular integrations on the right-hand side can be performed using Hecke's theorem[11]. (All formulas necessary for carrying out the angular integration are given in the appendix of Ref. 10.) The coefficients of $\Psi_1^{(+)}(\theta_1,\theta_2,\phi)$ and $\Psi_2^{(+)}(\theta_1,\theta_2,\phi)$ must vanish independently, yielding the following two separated, coupled equations that depend on the single variable $|p|$:

$$\begin{aligned}
&\left[|p|^2 + (1+\Delta)^2\right]\left[(1-\Delta)F^{(+)}(|p|) + |p|G^{(+)}(|p|)\right] \\
&\quad = -\frac{q_f Q_s}{(2\pi)^4}|p|\int_0^{\infty}\mathrm{d}|q|\,|q|^3\Lambda_{k_1+1/2}^{(2)}(|p|,|q|)G^{(+)}(|q|) \\
&\qquad -\frac{q_f Q_s}{(2\pi)^4}\int_0^{\infty}\mathrm{d}|q|\,|q|^4\Lambda_{k_1-1/2}^{(2)}(|p|,|q|)G^{(+)}(|q|)
\end{aligned} \tag{12a}$$

$$\begin{aligned}\left[|p|^2+(1+\Delta)^2\right]&\left[-|p|F^{(+)}(|p|)+(1-\Delta)G^{(+)}(|p|)\right]\\&=\frac{q_fQ_s}{(2\pi)^4}|p|\int_0^\infty \mathrm{d}|q|\,|q|^3\Lambda^{(2)}_{k_1-1/2}(|p|,|q|)F^{(+)}(|q|)\\&\quad+\frac{q_fQ_s}{(2\pi)^4}\int_0^\infty \mathrm{d}|q|\,|q|^4\Lambda^{(2)}_{k_1+1/2}(|p|,|q|)F^{(+)}(|q|)\end{aligned}\tag{12b}$$

In the above equation

$$\Lambda^{(2)}_n(|p|,|q|)=\frac{2\pi^2}{|p||q|}\,\frac{R(|p|,|q|)^{n+1}}{n+1}\,,\tag{13}$$

where

$$R(|p|,|q|)=\begin{cases}\frac{|q|}{|p|} & \text{if}\quad |q|\le|p|\,,\\ \\ \frac{|p|}{|q|} & \text{if}\quad |q|\ge|p|\,.\end{cases}\tag{14}$$

The index $k_1=1/2,3/2,\ldots$, and the angular momentum j of the bound state satisfies $j\le k_1$.

When $\chi(ip^0,\mathbf{p})$ with lower superscripts in (9) is substituted into the Bethe-Salpeter equation (5), the two equations that are obtained are identical to (12) after making the substitutions $F^{(-)}(|p|)\to F^{(+)}(|p|)$ and $G^{(-)}(|p|)\to -G^{(+)}(|p|)$. Since no additional eigenvalues are obtained by considering this second set of equations, attention is restricted to (12), and the superscripts $(+)$ are dropped for $F^{(+)}(|p|)$ and $G^{(+)}(|p|)$.

4. Analytical Boundary Conditions

The boundary conditions satisfied by the solutions as $|p|$ approaches zero and infinity must be determined before solutions can be calculated numerically. That is, the convergence parameters f_0, g_0, f_∞ and g_∞ must be determined that, respectively, satisfy the equations

$$F(|p|)\underset{|p|\to 0}{\longrightarrow}F_0|p|^{f_0}\,,\qquad G(|p|)\underset{|p|\to 0}{\longrightarrow}G_0|p|^{g_0}\,,\tag{15}$$

$$F(|p|)\underset{|p|\to \infty}{\longrightarrow}F_\infty|p|^{-f_\infty}\,,\qquad G(|p|)\underset{|p|\to \infty}{\longrightarrow}G_\infty|p|^{-g_\infty}\,,\tag{16}$$

where F_0, G_0, F_∞ and G_∞ are constants. The solutions for f_0 and g_0 were determined in Ref. 5 and are given by

$$f_0=k_1-\frac{1}{2}\,,\qquad g_0\ge k_1+\frac{1}{2}\,.\tag{17}$$

At large momenta the Bethe-Salpeter equation can be solved analytically. Each solution yields (a) an equation for the convergence parameters f_∞ or g_∞ in terms of the coupling constant and (b) an algebraic equation that expresses one of the convergence parameters in terms of the other. But the analytical solutions at large momenta only determine allowed ranges for the values of the convergence parameters, not the specific values for which there are solutions (at all momenta).

Among the five possible classes of solutions found in Ref. 5, solutions were found only for "Boundary Solutions I" where f_∞ and g_∞ satisfy the following conditions:

$$f_\infty=-k_1+\frac{5}{2}+\epsilon_f\,,\qquad 0<\epsilon_f<2\,k_1+1\,,\tag{18a}$$

$$g_\infty=-k_1+\frac{7}{2}+\epsilon_g\,,\qquad 0<\epsilon_g<2\,k_1+1\,,\tag{18b}$$

$$\epsilon_g\le\epsilon_f\le\epsilon_g+2\,.\tag{18c}$$

The four integrals in (12) can be evaluated analytically at large momentum $|p|$[12]. In this limit (12a) and (12b) can then be written, respectively, as

$$\begin{aligned}
&(1-\Delta)F_\infty\,|p|^{k_1-\frac{1}{2}-\epsilon_f}+G_\infty\,|p|^{k_1-\frac{1}{2}-\epsilon_g}\\
&\underset{|p|>>1}{=}-\frac{q_fQ_s}{4\pi}\frac{1}{\pi}\left[\frac{2(1+\epsilon_g)\,G_\infty}{\epsilon_g(2k_1+1-\epsilon_g)(2+\epsilon_g)}|p|^{k_1-\frac{1}{2}-\epsilon_g}\right.\\
&\qquad\left.+\frac{1}{2}\left(\frac{c_{g1}}{k_1+\frac{3}{2}}+\frac{c_{g2}}{k_1+\frac{1}{2}}\right)|p|^{-k_1-\frac{3}{2}}\right], \qquad (19a)\\
&-F_\infty\,|p|^{k_1+\frac{1}{2}-\epsilon_f}+(1-\Delta)G_\infty|p|^{k_1-\frac{3}{2}-\epsilon_g)}\\
&\underset{|p|>>1}{=}\frac{q_fQ_s}{4\pi}\frac{1}{\pi}\left[\frac{2(2k_1+2-\epsilon_f)F_\infty}{\epsilon_f(2k_1+1-\epsilon_f)(2k_1+3-\epsilon_f)}|p|^{k_1+\frac{1}{2}-\epsilon_f}+\frac{c_{f1}}{2(k_1+\frac{1}{2})}|p|^{-k_1-\frac{1}{2}}\right], \qquad (19b)
\end{aligned}$$

where c_{g1}, c_{g2} and c_{f1} are constants.

From (18c) there are four possible relationships between ϵ_f and ϵ_g: either $\epsilon_g < \epsilon_f$ or $\epsilon_g = \epsilon_f$ and either $\epsilon_f < \epsilon_g+2$ or $\epsilon_f = \epsilon_g+2$. In this talk attention is restricted to the case where boundary conditions allow coupling constants with magnitudes on the order of the fine structure constant α only when the bound states have spin-1/2:

$$\epsilon_f > \epsilon_g\,, \qquad \epsilon_f < \epsilon_g + 2\,. \qquad (20)$$

At very large momenta (19a) simplifies by noting that (20) implies $|p|^{k_1-\frac{1}{2}-\epsilon_f} \ll |p|^{k_1-\frac{1}{2}-\epsilon_g}$ and (18b) implies $|p|^{-k_1-\frac{3}{2}} \ll |p|^{k_1-\frac{1}{2}-\epsilon_g}$. Thus the terms proportional to $|p|^{k_1-\frac{1}{2}-\epsilon_f}$ and $|p|^{-k_1-\frac{3}{2}}$ can be neglected yielding

$$G_\infty|p|^{k_1-\frac{1}{2}-\epsilon_g}=-\frac{q_fQ_s}{4\pi}\frac{1}{\pi}\left[\frac{2(1+\epsilon_g)}{\epsilon_g(2k_1+1-\epsilon_g)(2+\epsilon_g)}\right]G_\infty|p|^{k_1-\frac{1}{2}-\epsilon_g}\,, \qquad (21)$$

or

$$\frac{q_fQ_s}{4\pi}=-\pi\frac{\epsilon_g(2k_1+1-\epsilon_g)(2+\epsilon_g)}{2(1+\epsilon_g)}\,. \qquad (22)$$

Similarly at very large momenta (19b) simplifies: from (20) and (18a) it follows, respectively, that $|p|^{k_1-\frac{3}{2}-\epsilon_g} \ll p|^{k_1+\frac{1}{2}-\epsilon_f}$ and $|p|^{-k_1-\frac{1}{2}} \ll p|^{k_1+\frac{1}{2}-\epsilon_f}$. Thus

$$-F_\infty|p|^{k_1+\frac{1}{2}-\epsilon_f}=\frac{q_fQ_s}{4\pi}\frac{1}{\pi}\left[\frac{2(2k_1+2-\epsilon_f)}{\epsilon_f(2k_1+1-\epsilon_f)(2k_1+3-\epsilon_f)}\right]F_\infty|p|^{k_1+\frac{1}{2}-\epsilon_f} \qquad (23)$$

or

$$\frac{q_fQ_s}{4\pi}=-\pi\frac{\epsilon_f(2k_1+1-\epsilon_f)(2k_1+3-\epsilon_f)}{2(2k_1+2-\epsilon_f)}\,. \qquad (24)$$

Equating (22) and (24) yields the following relationship between ϵ_f and ϵ_g:

$$\frac{\epsilon_g(2k_1+1-\epsilon_g)(2+\epsilon_g)}{(1+\epsilon_g)}=\frac{\epsilon_f(2k_1+1-\epsilon_f)(2k_1+3-\epsilon_f)}{(2k_1+2-\epsilon_f)} \qquad (25)$$

If ϵ_f is specified, then (25) becomes a cubic equation for ϵ_g that is easily solved when written in the factored form

$$0=(\epsilon_g+\epsilon_f-2k_1-1)[\epsilon_g^2(-\epsilon_f+2k_1+2)+\epsilon_g(\epsilon_f-2)(\epsilon_f-2k_1-2)+\epsilon_f(\epsilon_f-2k_1-3)] \qquad (26)$$

The solutions are

$$\epsilon_g = 2k_1 + 1 - \epsilon_f \, , \tag{27a}$$

$$\epsilon_g = \frac{1}{2}\left[\epsilon_f - 2 \pm \sqrt{\frac{8(k_1+1) + 2(k_1+1)\epsilon_f^2 - \epsilon_f^3}{2(k_1+1) - \epsilon_f}}\,\right] . \tag{27b}$$

Expressing ϵ_g in terms of ϵ_f greatly simplifies the numerical search for solutions: instead of independently searching for solutions with values of ϵ_f and ϵ_g in their allowed ranges (18), it is only necessary to search for solutions with values of ϵ_f in its allowed region $0 < \epsilon_f < 2k_1 + 1$.

The constituents in a composite model of leptons and quarks would likely have charges with magnitudes on the order of e, or coupling constants with magnitudes on the order of the fine structure constant $\alpha = e^2/(4\pi) \simeq 1/137$. From (22) and (24), respectively, the magnitude of the coupling constant is small when either ϵ_g or $2k_1 + 1 - \epsilon_g$ is small and when either ϵ_f or $2k_1 + 1 - \epsilon_f$ is small. Solutions are normalizable only if they decrease faster than $|p|^{-3}$ at large momenta[5]. When ϵ_g is small, from (18b) solutions are normalizable only when $k_1 = 1/2$, implying that all possible solutions have spin-1/2. When ϵ_f is small, from (18a), the solution is not normalizable. Thus there are two cases where the boundary conditions allow normalizable solutions with small coupling constants: (a) When ϵ_g and $2k_1+1-\epsilon_f$ are small, (27a) is satisfied. Boundary conditions exist that are compatible with small coupling constants, and any solutions have spin-1/2. When $2k_1 + 1 - \epsilon_g$ and $2k_1 + 1 - \epsilon_f$ are small, (27b) is satisfied. Boundary conditions allow higher-spin solutions.

5. Numerical procedure for solving the bound-state Bethe-Salpeter equation

Although solving the two-body, bound-state Schrödinger equation numerically is significantly easier than solving the two-body, bound-state Bethe-Salpeter equation, the general method for solving both is the same. The two-body, bound-state Schrödinger equation (3) can be solved in two steps:

Step # 1: The solution $\psi(\mathbf{x})$ is expanded in terms of a finite set of basis functions $\{b_j(\mathbf{x})\}$,

$$\psi(\mathbf{x}) = \sum_{j=1}^{N} c_j b_j(\mathbf{x}) \, . \tag{28}$$

Using only a finite number of basis functions in the above expansion is a necessary approximation when carrying out a numerical calculation. By increasing the number of basis functions, the approximation is improved so that increasingly accurate solutions are obtained. Substituting the expansion for $\psi(\mathbf{x})$ into the Schrödinger equation (3),

$$\sum_{j=1}^{N} H(\mathbf{x}) b_j(\mathbf{x}) c_j = E \sum_{j=1}^{N} b_j(\mathbf{x}) c_j \, . \tag{29}$$

Step # 2: The eigenvalue equation is discretized and solved numerically by converting it into a generalized matrix eigenvalue equation using the Rayleigh-Ritz-Galerkin variational method[13, 14]: Multiplying both sides of the above equation by $b_i^\dagger(\mathbf{x})$ and integrating over $\mathbf{x}$,

$$\sum_{j=1}^{N} \int_{-\infty}^{\infty} \mathrm{d}^3x \, b_i^\dagger(\mathbf{x}) H(\mathbf{x}) b_j(\mathbf{x}) c_j = E \sum_{j=1}^{N} \int_{-\infty}^{\infty} \mathrm{d}^3x \, b_i^\dagger(\mathbf{x}) b_j(\mathbf{x}) c_j \, . \tag{30}$$

In (30) the Schrödinger equation has been rewritten as a $N \times N$ generalized matrix eigenvalue equation of the form

$$Ac = E\; Bc, \tag{31}$$

where the matrices A and B are given, respectively, by

$$A_{i\,j} = \int_{-\infty}^{\infty} \mathrm{d}^3x\, b_i^\dagger(\mathbf{x}) H(\mathbf{x}) b_j(\mathbf{x})\,, \qquad B_{i\,j} = \int_{-\infty}^{\infty} \mathrm{d}^3x\, b_i^\dagger(\mathbf{x}) b_j(\mathbf{x})\,. \tag{32}$$

All eigenvalues of a generalized matrix eigenvalue equation of the form (31) are real if A and B are Hermitian and if A, B or both are positive definite.

Although numerical solutions are obtained by discretizing the Schrödinger equation, the solutions of the discretized Schrödinger equation can be used to construct solutions to the Schrödinger equation itself. The eigenvalues E of the discretized equation are also the eigenvalues of the Schrödinger equation. Furthermore, the eigenvector $c = (c_1, c_2, \dots)$ of the discretized equation (31) is the set of expansion coefficients for the solution $\psi(\mathbf{x})$ in (28) of the Schrödinger equation (3).

The Bethe-Salpeter equation is solved similarly to the separated Schrödinger equation with three complicating factors:
(a) As can be seen from the Bethe-Salpeter equation (2), the kernel of the equation - and thus the solutions - are singular as a result of propagators in Minkowski space. The singularities are eliminated by rewriting the equation in Euclidean space[6].
(b) It is possible to discretize the Bethe-Salpeter equation and obtain a generalized matrix eigenvalue equation of the form

$$\text{Discretized Bethe-Salpeter Equation: } Ac = \frac{q_f Q_s}{4\pi}\, B\,. \tag{33}$$

Because a relativistic Hamiltonian does not exist, it is not usually possible to discretize the equation so that all eigenvalues are real. That is, it is not possible to create a generalized matrix eigenvalue equation of the form (33) where the matrices A and B are Hermitian and at least one is positive definite. However, solutions with real eigenvalues are obtained when the basis functions obey the boundary conditions.
(c) For the bound-state Bethe-Salpeter equation (2) that might describe leptons and quarks as bound states, the coupling constant determines the behavior of the solution at large momenta, which are boundary conditions. The boundary conditions at large momenta can be obtained analytically because the Bethe-Salpeter equation can be solved analytically in this limit. The discretized Bethe-Salpeter equation is non-linear in the coupling constant since the coupling constant appears both in the Bethe-Salpeter equation as the eigenvalue and in the basis functions.

Only spin-1/2 solutions are calculated. Since the angular momentum j satisfies $j \le k_1$, the index $k_1 = 1/2$. Spin-1/2 solutions are somewhat less difficult to calculate than higher-spin solutions and are the most interesting since, if leptons and quarks are composite, they would be spin-1/2 bound states.

The zero-energy solutions $F(|p|)$ and $G(|p|)$ in (12) are expanded in terms of basis functions as follows:

$$F(|p|) = \frac{|p|^{f_0}}{(|p|+1)^{f_0+2+\epsilon_f}} \sum_{j=1}^{N} f_j B_j\,, \tag{34a}$$

$$G(|p|) = \frac{|p|^{g_0}}{(|p|+1)^{g_0+3+\epsilon_g}} \sum_{j=1}^{N} g_j B_j\,. \tag{34b}$$

In (34) f_0 and g_0 are given in (17), and from (18) $f_\infty = 2 + \epsilon_f$ and $g_\infty = 3 + \epsilon_g$. Thus the factor preceding each summation symbol obeys the boundary conditions that $F(|p|)$ or $G(|p|)$, respectively, obey. The B_j are given by

$$B_j = \begin{cases} \text{cubic spline} & \text{for} \quad j = 1, \ldots, N-4\,, \\ \\ \text{boundary spline} & \text{for} \quad j = N-3 \ldots N\,. \end{cases} \tag{35}$$

Cubic splines[15] are cubic polynomials that, along with their first two derivatives, are continuous. Cubic splines, one of which is depicted in Fig. 2(a), are nonzero on four contiguous intervals labeled #1, #2, #3 and #4.

At large momenta solutions are expanded in terms of boundary splines. Boundary splines and their first two derivatives are everywhere continuous. In addition, as the momentum approaches infinity, the boundary splines become constants. As a consequence all basis functions, and, therefore, all solutions obey the boundary conditions at large momenta. An example of each of the four types of boundary splines is depicted in Fig. 2(b).

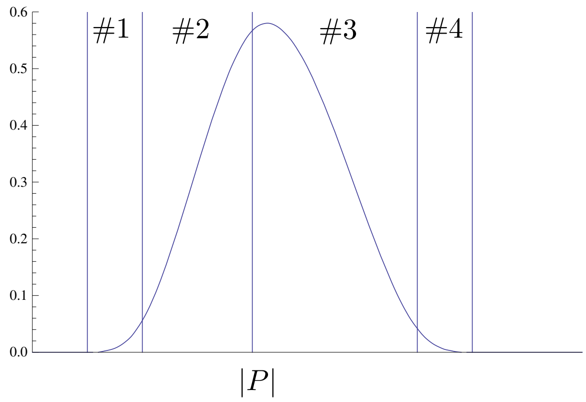

(a) Cubic Spline

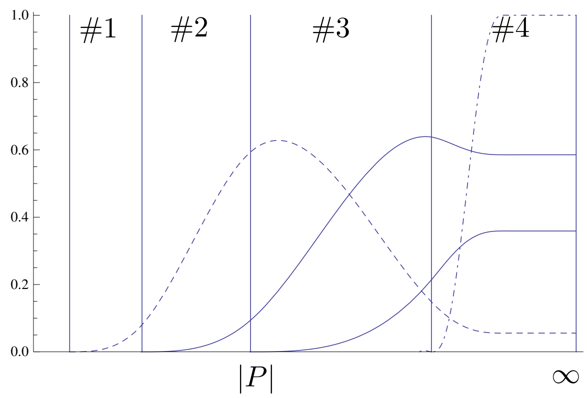

(b) Boundary Splines

Figure 2.

Because the discretized, Bethe-Salpeter equation is non-linear in the coupling constant, it is solved by systematically sweeping through the allowed values of ϵ_f in the range specified by (18a). The value of ϵ_g is then calculated from (27), and the input value of the coupling constant $q_f Q_s/(4\pi)_{\text{input}}$ is calculated from either (22) or (24). The coupling constant $q_f Q_s/(4\pi)_{\text{ouput}}$ is calculated as an eigenvalue of the discretized Bethe-Salpeter equation. When the quantity $[q_f Q_s/(4\pi)_{\text{input}} - q_f Q_s/(4\pi)_{\text{ouput}}]$ changes sign, a value of the coupling constant that is a solution to the Bethe-Salpeter equation lies between the two input values of the coupling constant that yield different signs for $[q_f Q_s/(4\pi)_{\text{input}} - q_f Q_s/(4\pi)_{\text{ouput}}]$.

6. Numerical solutions of the bound-state Bethe-Salpeter equation

The only solutions found satisfy (27a), namely, $\epsilon_f + \epsilon_g = 2.00$. In Fig. 3 the coupling constant $q_f Q_s/(4\pi)$ is plotted as a function of the dimensionless mass parameter Δ.

It is possible to understand why the coupling constant $q_f Q_s/(4\pi)$ plotted in Fig. 3 is weakly dependent on Δ. As discussed in §4, the behavior of the solutions at large $|p|$ determines the

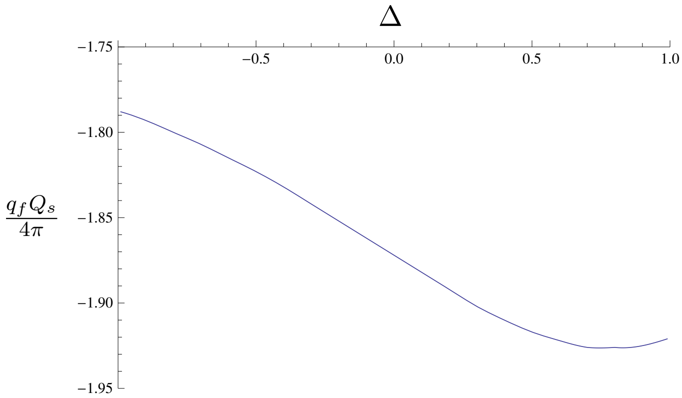

Figure 3. The coupling constant $q_f Q_s/(4\pi)$ as a function of the dimensionless mass parameter Δ when $j = 1/2$ and $E = 0$.

coupling constant. At large $|p|$ (12a) and (12b) become, respectively,

$$|p|^3\, G(|p|) \underset{|p|>>1}{=} -\frac{q_f Q_s}{(2\pi)^4}\int_0^\infty |q|^3 \Big[|p|\Lambda^{(2)}_{k_1+1/2}(|p|,|q|) + |q|\Lambda^{(2)}_{k_1-1/2}(|p|,|q|)\Big]\, G(|q|)\mathrm{d}|q|\,, \tag{36a}$$

$$|p|^3\, F(|p|) \underset{|p|>>1}{=} -\frac{q_f Q_s}{(2\pi)^4}\int_0^\infty |q|^3 \Big[|p|\Lambda^{(2)}_{k_1-1/2}(|p|,|q|) + |q|\Lambda^{(2)}_{k_1+1/2}(|p|,|q|)\Big]\, F(|q|)\mathrm{d}|q|\,. \tag{36b}$$

As can be seen from (36), at large $|p|$ the Bethe-Salpeter equation does not depend explicitly on Δ. But because Δ occurs in (11), when $|p|$ is small $F(|p|)$ and $G(|p|)$ depend significantly on Δ. For large $|p|$, $F(|p|)$ and $G(|p|)$ depend only implicitly on Δ through integrals over $F(|p|)$ and $G(|p|)$. That dependence is sufficiently small that the coupling constant depends weakly on Δ.

In Fig. 4 the components $F(|p|)$ and $G(|p|)$ of the solution are plotted as a function of $|p|$ when the mass parameter $\Delta = 0.8$, implying $m_f/m_s = 1/9$. A solution is found for $\epsilon_f = 1.52$, which implies that $\epsilon_g = 0.483$ and $q_f Q_s/(4\pi) = -1.93$. When m_f/m_s is substantially less than 1, as can be seen from Fig. 4, $F(|p|)$, which is the pure angular momentum $\ell = 0$ component, and $G(|p|)$, which is a mixed angular momentum $\ell = 0$ and $\ell = 1$ component, are roughly comparable in magnitude.

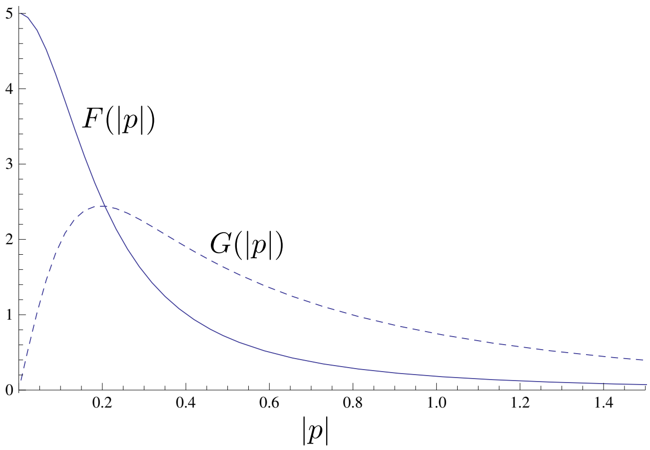

Figure 4. The components $F(|p|)$ and $G|p|)$ of a solution as a function of $|p|$ for $m_f/m_s = 1/9$, $\epsilon_f = 1.52$, $\epsilon_g = 0.483$ and $q_f Q_s/(4\pi) = -1.93$.

As the mass ratio m_f/m_s increases, however, the magnitude of the pure $\ell = 0$ component $F(|p|)$ becomes much larger than the magnitude of the mixed $\ell = 0$ and $\ell = 1$ component $G(|p|)$. In Fig. 5(a) the component $G(|p|)$ of a solution is plotted as a function of $|p|$ when the mass parameter $\Delta = -0.8$ or $m_f/m_s = 9$ and $\epsilon_f = 1.57$, implying that $\epsilon_g = 0.429$ and

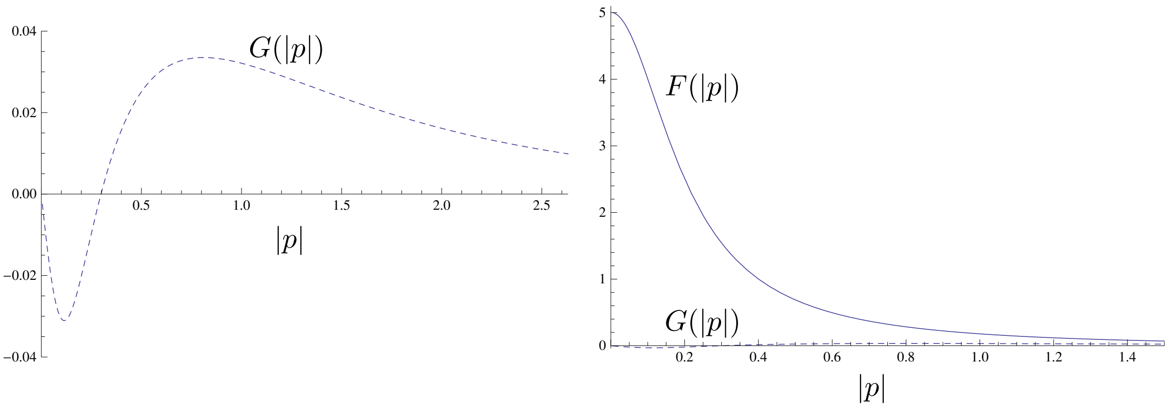

(a) (b)

Figure 5. (a) The component $G|p|)$ and (b) the components $F(|p|)$ and $G|p|)$ of the same solution as a function of $|p|$ for $m_f/m_s = 9$, $\epsilon_f = 1.57$, $\epsilon_g = 0.429$ and $q_f Q_s/(4\pi) = -1.80$.

$q_f Q_s/(4\pi) = -1.80$. To provide a visual comparison of $F(|p|)$ and $G(|p|)$, both are plotted as a function of $|p|$ in Fig. 5(b). The magnitude of $G(|p|)$ is so much smaller than the magnitude of $F(|p|)$ that the dashed line depicting $G(|p|)$ is barely visible. If two spin-1/2, bound states are both pure $\ell = 0$ states, the first-order, electromagnetic decay of one into the other is forbidden by conservation of angular momentum. Thus if two states have large values of m_f/m_s, the first-order electromagnetic decay of one into the other is strongly suppressed.

7. Checking numerical solutions

Solutions calculated from the generalized matrix eigenvalue equation (33) are checked in the following ways: (a) As the number of basis functions is increased, the value of each eigenvalue must converge. (b) For each solution the left- and right-hand sides of the Bethe-Salpeter equation are compared in the physical region on a set of points spanning the space. The values of the left- and right-hand sides of the equation are written at the points where the absolute errors between the two sides of the equation are greatest. For solutions with $|\Delta| \leq 0.8$ the greatest percent difference between points with the largest absolute difference between the left- and right-hand sides of the equation is less than 0.08%. For $0.8 < |\Delta| < 0.95$, the percent difference increases substantially and is always only less than 4.6% although the left-and right-hand sides agree much more closely at almost all points. (c) The left-and right-hand sides of the equation must very nearly agree at the largest values of momenta. At the largest value of dimensionless momentum sampled, $|p| = 1.50 \times 10^8$, the maximum percent difference between the left- and right-hand sides of (12) is 3×10^{-3}% for $-0.99 \leq \Delta \leq 0.99$. (d) A reliability coefficient $r_{lhs-rhs}$[16], which is a statistical measure of how closely the left- and right-hand sides of (12) agree at the sampled points, is calculated. If the left- and right-hand sides agree exactly at every point, then $r_{lhs-rhs} = 1$. Except when $\Delta = -0.99$ calculations are refined until the reliability coefficient for each solution equals 1 to ten significant figures. (e) A second reliability coefficient $r^{\text{final}}_{lhs-rhs}$ is calculated for the final N_{large} points that are sampled at large momenta. Calculations are always refined until the reliability coefficient for each solution equals 1 to ten significant figures.

8. Conclusions and future research

Strongly bound states with coupling constants with magnitudes on the order of the electromagnetic fine structure constant α are allowed by the boundary conditions and may exist. In the ladder approximation as the magnitude of coupling constant is decreased from 1.00

to the fine structure constant α, the input and output values of the coupling constant always have the same sign, implying that there are no solutions. However, when the magnitude of the input value of the coupling constant is α, the input and output values of the coupling constant differ by $4 \times 10^{-3}\%$, The additional attractive force created by the seagull and crossed fourth-order diagrams may be sufficient to create strongly bound states with a coupling constant on the order of $-\alpha$. The author is currently calculating these effects. For the class of solutions discussed here, all such strongly bound states would have spin-1/2 as do the leptons and quarks. Finally, a mechanism exists to suppress the decay $\mu \to e + \gamma$.

Acknowledgments
This work was supported by an allocation of computing time from the Ohio Supercomputer Center.

References

[1] Smolin L 2006 *The Trouble with Physics* (Boston: Houghton Mifflin Co.)
[2] Bennett G W *et al.* 2004 *Physical Review Letters* **92** 161802
[3] Bjorken J D and Drell S D 1965 *Relativistic Quantum Fields* (New York: McGraw Hill)
[4] Salpeter E E and Bethe H A 1951 *Physical Review* **84** 1232
[5] Mainland G B 2008 *Prog. Theor. Phys.* **119** 263
[6] Wick G C 1954 *Physical Review* **96** 1124
[7] Cutkosky R E 1954 *Physical Review* **96** 1135
[8] Mainland G B 2004 *Computat. Physics* **197** 610
[9] Sugano R and Munakata Y 1956 *Prog. Theor. Phys.* **16** 532
[10] Mainland G B 1986 *J. Math. Phys.* **27** 1344
[11] Hecke E 1918 *Math. Ann.* **78** 398
[12] Mainland G B 2003 *Few-Body Systems* **33** 71
[13] Delves L M and Walsh J 1974 *Numerical Solution of Integral Equations* (Oxford: Clarendon Press)
[14] Atkinson K E 1976 *A Survey of Numerical Methods for the Solution of Fredholm Integral Equations of the Second Kind* (Philadelphia: SIAM)
[15] de Boor C 1978 *A Practical Guide to Splines* (Berlin: Springer-Verlag)
[16] Winer B J 1962 *Statistical Principles in Experimental Design* (New York: McGraw Hill)